J. Phycol. **50,** 140–148 (2014)
© 2013 Phycological Society of America
DOI: 10.1111/jpy.12147

GENETIC DELINEATION BETWEEN AND WITHIN THE WIDESPREAD COCCOLITHOPHORE MORPHO-SPECIES *EMILIANIA HUXLEYI* AND *GEPHYROCAPSA OCEANICA* (HAPTOPHYTA)[1]

El Mahdi Bendif[2]

CNRS UMR7144/UPMC, EPEP team, Station Biologique de Roscoff, Roscoff 29682, France
Marine Biological Association of the United Kingdom, Citadel Hill, Plymouth, Devon PL1 2PB, UK

Ian Probert

CNRS/UPMC, FR2424, Station Biologique de Roscoff, Roscoff 29682, France

Margaux Carmichael, Sarah Romac

CNRS UMR7144/UPMC, EPEP team, Station Biologique de Roscoff, Roscoff 29682, France

Kyoko Hagino

Institute for Study of the Earth's Interior Okayama University, 827 Yamada, Misasa, Tottori 682-0193, Japan

and Colomban de Vargas

CNRS UMR7144/UPMC, EPEP team, Station Biologique de Roscoff, Roscoff 29682, France

***Emiliania huxleyi* and *Gephyrocapsa oceanica* are abundant coccolithophore morpho-species that play key roles in ocean carbon cycling due to their importance as both primary producers and calcifiers. Global change processes such as ocean acidification impact these key calcifying species. The physiology of *E. huxleyi*, a developing model species, has been widely studied, but its genetic delineation from *G. oceanica* remains unclear due to a lack of resolution in classical genetic markers. Using nuclear (18S rDNA and 28S rDNA), mitochondrial (*cox1*, *cox2*, *cox3*, *rpl16*, and *dam*), and plastidial (16S rDNA, *rbcL*, *tufA*, and *petA*) DNA markers from 99 *E. huxleyi* and 44 *G. oceanica* strains, we conducted a multigene/multistrain survey to compare the suitability of different markers for resolving phylogenetic patterns within and between these two morpho-species. The nuclear genes tested did not provide sufficient resolution to discriminate between the two morpho-species that diverged only 291Kya. Typical patterns of incomplete lineage sorting were generated in phylogenetic analyses using plastidial genes. In contrast, full morpho-species delineation was achieved with mitochondrial markers and common intra-morpho-species phylogenetic patterns were observed despite differing rates of DNA substitution. Mitochondrial genes are thus promising barcodes for distinguishing these coccolithophore morpho-species, in particular in the context of environmental monitoring.**

Key index words: **coccolithophore; DNA barcoding; *Emiliania huxleyi*; *Gephyrocapsa oceanica*; phylogeny; species complex**

Coccolithophores are widespread and abundant marine microalgae characterized by their covering of minute calcite platelets, the coccoliths. They have played key roles in global biogeochemical cycles (Rost and Riebesell 2004) since their origin in the Triassic (Bown 2005), and intense research interest has recently been focused on attempting to predict the responses of coccolithophores to environmental changes linked to the antropogenically induced rise in atmospheric CO_2, (i.e., effects such as global warming and ocean acidification; Riebesell et al. 2000, Iglesias-Rodriguez et al. 2008, Langer et al. 2009). The fossil remains of coccolithophores also provide valuable proxies for paleo-environment reconstruction, both via elemental and isotopic analysis of coccoliths (e.g., Candelier et al. 2013) and via measurement of the ratio of different types of alkenone, a class of robust long-chain (C_{37}-C_{39}) esters of polyunsaturated n-C_{36} acids and C_{27}-C_{29} sterols produced uniquely by members of the coccolithophore order Isochrysidales and widely used as a proxy for sea surface temperature (Müller et al. 1998).

The two numerically most important extant coccolithophores are *Emiliania huxleyi* Lohmann (Lohmann 1902) and *Gephyrocapsa oceanica* Kamptner (Kamptner 1943). *Emiliania huxleyi* is cosmopolitan in world oceans and frequently forms

[1]Received 30 January 2013. Accepted 13 October 2013.
[2]Author for correspondence: e-mail elmben@mba.ac.uk.
Editorial Responsibility: T. Mock (Associate Editor)

extensive "milky water" blooms in high latitude coastal and shelf ecosystems (Winter et al. 1994), while *G. oceanica* is a warm water species that occasionally blooms in transitional coastal waters in the Pacific ocean (e.g., Blackburn and Cresswell 1993, Kai et al. 1999). These sister species belong to the family Noëlaerhabdaceae within the prymnesiophyte order Isochrysidales and exhibit almost identical coccolith structure. They are distinguished by their relative degree of calcification, with notably the elevation of two of the central tube crystals forming a disjunct bridge over the central area of coccoliths in *Gephyrocapsa* (Fig. S1 in the Supporting Information). *E. huxleyi* coccoliths first appeared in the fossil record only 291,000 years ago (Raffi et al. 2006) and fossil evidence suggests that *E. huxleyi* evolved directly from *G. oceanica* (Samtleben 1980).

Different clonal culture strains of *E. huxleyi* have been reported to respond differently in terms of calcification to acidification of the growth medium (Riebesell et al. 2000, Iglesias-Rodriguez et al. 2008, Langer et al. 2009), raising the question as to whether distinct genetic entities (cryptic or pseudocryptic species) exist within this morphologically defined species. Comparison of classical nuclear ribosomal gene markers provides little or no resolution between *E. huxleyi* and *G. oceanica* (Edvardsen et al. 2000, Fujiwara et al. 2001, Liu et al. 2010), but there is preliminary evidence for genetic separation between the two morpho-species and/or within *E. huxleyi* from genetic markers including the nuclear-encoded calcium binding protein *GPA* gene (Schroeder et al. 2005), the plastid-encoded elongation factor *tuf*A gene (Medlin et al. 2008, Cook et al. 2011) and the mitochondrial cytochrome c oxidase subunit 1 (*cox1*) gene (Hagino et al. 2011). These studies were conducted with different (and generally small) sets of culture strains, and different markers appear to give different phylogenetic patterns in relation to morphology and biogeographical origin of strains. In addition, in some cases the two morpho-species are only partially separated by the genetic marker (e.g., the *tuf*A analysis of Medlin et al. 2008).

In this context, we used a relatively large set of culture strains to test a variety of genetic markers from different cellular compartments for their ability to distinguish genotypes between and within *E. huxleyi* and *G. oceanica* and for their suitability for performing phylogenetic reconstructions. In addition to the classical (but relatively slowly evolving) nuclear *18S* and *28S* ribosomal DNA (rDNA) and plastidial *rbcL* markers, we chose to extend previous analyses of *tuf*A and *cox1* and to include a comparison of other markers such as the plastid-encoded *16S* rDNA (widely used in prokaryote phylogenetics and increasingly used for photosynthetic organisms), the plastid-encoded *pet*A gene (coding for a subunit of cytochrome f), and mitochon drion-encoded genes including two other cytochrome oxidase genes (*cox2*, *cox3*), and the *rpl16* (coding for a protein involved in the ribosomal large subunit) and *dam* (coding for a DNA adenine methylase) genes. Evaluation of these molecular tools represents an essential first step toward large-scale assessment, using next generation sequencing amongst other methods, of the biodiversity, biogeography, and eco-evolutionary dynamics of these key phytoplankton taxa.

MATERIALS AND METHODS

Origin and morphological characterization of culture strains. Clonal culture strains (Table S1 in the Supporting Information) from the Roscoff Culture Collection, the Plymouth culture collection, and the Provasoli-Guillard Center for Culture of Marine Phytoplankton were maintained in K/2(-Si,-Tris,-Cu) medium (Keller et al. 1987) at 17°C with 50 μmol photons $\cdot$ m^{-2} $\cdot$ s^{-1} illumination provided by daylight neon tubes with a 14:10 h L:D cycle. For analysis of coccolith morphology by SEM, calcified cells were harvested at early exponential growth phase and filtered onto 0.22 μm nucleopore filters (Millipore, Molsheim, France), then dried for 2 h at 55°C. Small pieces of filters were gold/palladium sputter coating and observed with a FEI Quanta SEM (FEI, Hillsboro, OR, USA).

DNA extraction, amplification, and sequencing. Genomic DNA was extracted from cultures harvested in the exponential phase of growth using the DNeasy Plant mini kit (Qiagen, Hilden, Germany). Partial *18S, 28S, 16S, rbcL, tuf*A (two fragments, one short and one long), *pet*A, *cox1* (two fragments, one short, and one long), *cox2, cox3, rpl16,* and *dam* genes were amplified by PCR using the primer sets listed in Table S2 in the Supporting Information (primer maps are illustrated in Fig. S2 in the Supporting Information). PCRs were performed in a total reaction volume of 25 μL using the *Phusion* Polymerase kit (Finnzymes, Espoo, Finland). A standard PCR protocol was used for all genes with a T1 thermal cycler (Biometra, Göttingen, Germany): 2 min initial denaturation at 98°C, followed by 35 cycles of 10 s at 98°C, 30 s annealing at 55°C, 30 s extension at 72°C. A final 10 min extension step at 72°C was conducted to complete the amplification. Amplification products were controlled by electrophoresis on a 1% agarose gel. The PCR products were sequenced directly on an ABI PRISM 3100 xl DNA auto sequencer (Perkin-Elmer, Foster City, CA, USA) using the ABI PRISM BigDye Terminator Cycle Sequencing Kit (Perkin-Elmer). The sequences determined in this study were deposited in GenBank (Table S3 in the Supporting Information).

Sequence comparison and phylogenetic analyses. The nucleotide sequence data sets of each gene were aligned using the online version of the multiple alignment program MAFFT (Katoh et al. 2007). Alignments were double-checked de visu in the sequence editor BIOEDIT (Hall 1999) and coding regions were determined for plastidial (Sanchez-Puerta et al. 2005) and mitochondrial (Sánchez Puerta et al. 2004) markers. Sequences were compared using the Kimura 2-parameter distance with the MEGA 5 software (Tamura et al. 2011). To visualize genetic variability within and between morpho-species, analyses were performed with DnaSP v5.10 (Librado and Rozas 2009) estimated by *pi* (Nei 1987). Maximum likelihood and neigbor joining phylogenetic trees were inferred for each gene and for the concatenation of *28S* rDNA, *cox3,* and *tuf*A sequences using the MEGA 5 software. Appropriate models of DNA substitution were detected with MEGA 5, using the three proposed statistics (AIC, AICc, and BIC). For most markers, the best-fit substitution model was the HKY model

(Hasegawa et al. 1985), which distinguishes between transversion and transition rates with unequal base frequencies. For the *tuf*A short fragment data set, the K2P substitution model (Kimura 1980) was applied, differing from the HKY model by being based on equality of base frequencies, and for the *rpl16* data set, the TN model (Tamura and Nei 1993) allowed different rates for two transitions (A-G and C-T) and constant rates for transversions with unequal base frequencies. Tree topologies were statistically tested by bootstrapping based on 1,000 replicates for both methods.

RESULTS

Gene marker diversity. The partial sequences of the nuclear *18S* rDNA and the plastidial *16S* rDNA and *rbcL* were strictly identical for all strains of both morpho-species (Table 1), confirming that these genes are not suitable for discriminating between and within *E. huxleyi* and *G. oceanica*. Of the other genetic markers, the lowest value of nucleotide diversity (pi = 0.1×10^{-3}) was recorded with *28S* rDNA sequences with a consistent 1 base pair differentiation between the two morpho-species. All other gene markers tested in this study exhibited higher relative nucleotide substitution rates and polymorphisms, with the partial sequences of plastidial *tuf*A (long; 6.4%) and mitochondrial *dam* (6.0%) exhibiting the highest degrees of variability for the set of cultures analysed (pi = 14.7×10^{-3} and 15.6×10^{-3}, respectively; Table 1). While several of the markers tested exhibited sufficient variability to be potentially suitable for barcoding and/or phylogenetic applications, full distinction of *G. oceanica* from *E. huxleyi* was not achieved with certain genes. The variability within *tuf*A (long and short), *pet*A, and *cox1* (short) only partially delineated the two morpho-species, with interspecific overlap (i.e., polyphyly in phylogenetic reconstructions; Fig. 1). These markers exhibited a relatively high level of polymorphism (Table 1) highlighting microdiversity within each morpho-species. Previous studies using the plastid gene *tuf*A also reported that microdiversity could be revealed within *G. oceanica* and *E. huxleyi*, but that these morpho-species cannot be clearly distinguished with this marker (Medlin et al. 2008, Cook et al. 2011). By contrast, consistent interspecific delineation was attained with the mitochondrial *cox1* (long), *cox2*, *cox3*, *rpl16,* and *dam* markers. These mitochondrial markers also delineated consistent groups within *E. huxleyi*, strictly comparable to the biogeographically coherent clusters as defined by a longer mitochondrial fragment spanning the *cox1-atp4* genes (Hagino et al. 2011). The highest percentage of interspecific differentiation was attained with the *dam* gene (2.6%), that also exhibited the highest level of intraspecific divergence within *G. oceanica* (1.5%, equal to the divergence within this morpho-species shown by *pet*A despite a lower level of polymorphism (pi = 3.15×10^{-3} and 8.37×10^{-3} for *dam* and *pet*A, respectively; Table 1). The *dam* gene also exhibited the highest intraspe-

TABLE 1. Characteristics of genetic markers used in this study.

Compartment	Gene	Average length (bp)	Number sequences	GC content (%)	Codons (residues)	Number/ Percentage (%) of totale substitutions	Non-synonymous substitutions	Synonymous substitutions	Parsimonious informative site	Best model (AICc)	Genetic diversity (pi (10^{-3}))/ observed genetic distance (%)	Genetic diversity (pi (10^{-3}))/ Observed genetic distance (%) in *Gephyrocapsa oceanica*	Genetic diversity (pi (10^{-3}))/Observed genetic distance (%) in *Emiliania huxleyi*
Nucleus	*18S*	1721	40	60	–	0/0	–	–		–	0/0	0/0	0/0
	28S	631	51	62.1	–	1/0.2	–	–		–	0.7/0.1	0/0	0/0
Plastid	*16S*	700	16	51.2	–	0/0	–	–		HKY	0/0	0/0	0/0
	rbcL	522	16	45.6	174	0/0	–	–		–	0/0	0/0	0/0
	tufA (short)	240	59	43.7	80	6/2.9	1	5	4	K2P	4/-	3.3/0.3	4/0.6
	tufA (long)	637	18	37,9	212	26/6.4	9	15	24	HKY+G	14.7/-	8.4/1.2	14.9/1.2
	petA	417	29	41.2	139	21/5.3	3	19	10	HKY	7.2/-	7.6/1.5	6.6/1.1
Mitochondrion	*cox1* (short)	651	124	30,7	217	32/5.7	0	32	27	HKY+G	8.3/-	10.3/0.3	5.2/0.4
	cox1 (long)	903	50	32.2	301	53/4.4	4	49	38	HKY+I	9.3/1	8.8/0.6	4.9/0.4
	cox2	766	28	31.8	262	20/1.7	1	19	15	HKY+I	8/1.8	1.3/0.6	3.7/0.4
	cox3	810	104	34.6	270	38/4.2	4	34	30	HKY	11.3/2.1	0.5/0.1	5.9/0.9
	rpl16	326	37	29.8	108	14/4	3	11	10	TN+I	13.4/2.3	3.3/1	2.5/0.8
	dam	414	36	27.3	138	26/6	11	15	20	HKY	15.6/2.6	3.2/2.6	10.5/0.8

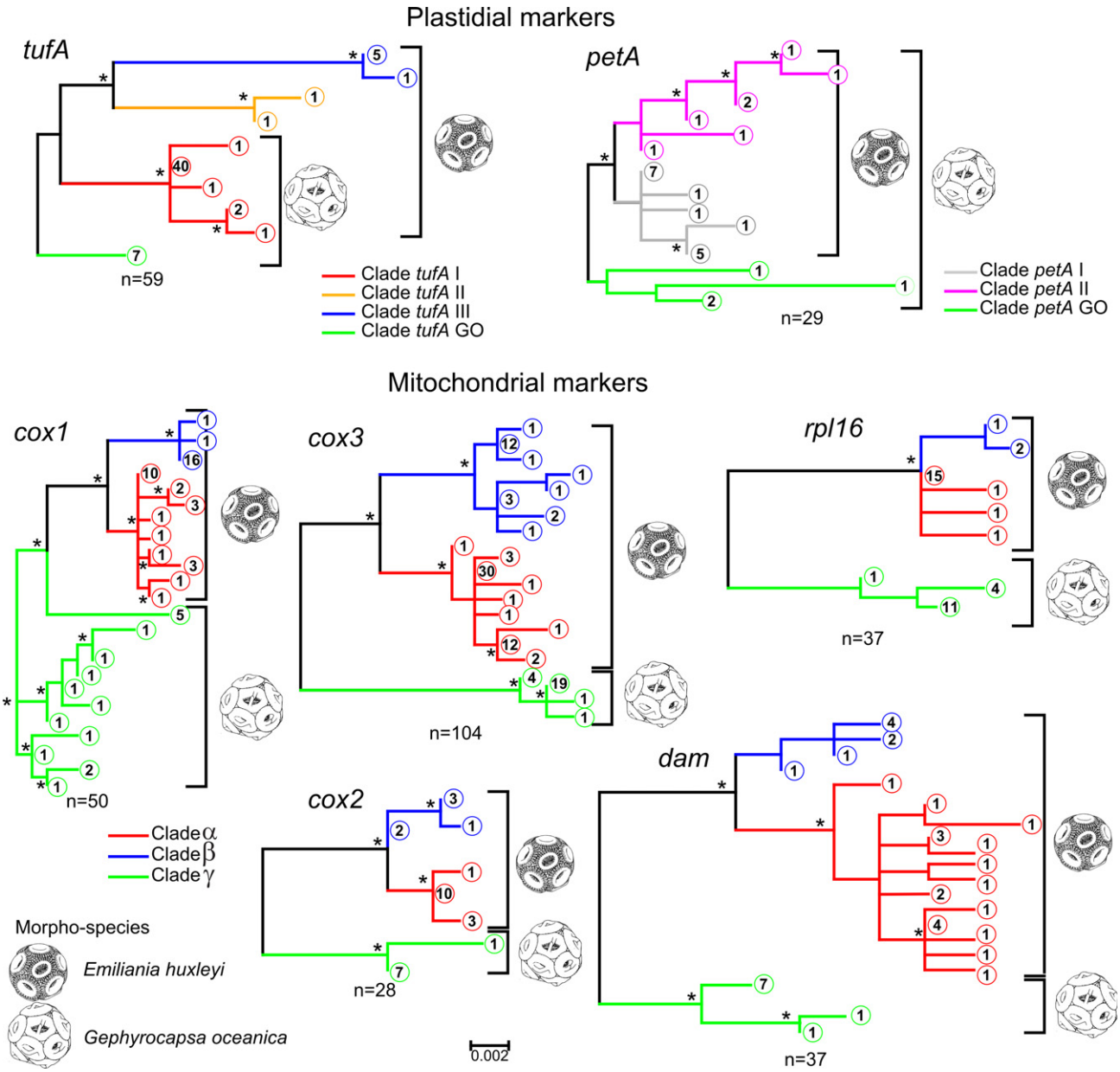

FIG. 1. Unrooted schematic phylogenetic trees inferred from genetic markers used in this study. The pattern of morpho-species delineation, indicated by *Emiliania huxleyi* and *Gephyrocapsa oceanica* drawings, summarizes SEM observations of all sequenced strains. For plastidial markers, clades were defined independently for each gene; for mitochondrial markers, clades α and β correspond to clades defined by Hagino et al. (2011). Number of sequences per tree and per branch is, respectively, given by the "n" at the bottom of each tree and the encircled number at each branch. Detailed phylogenetic position of each strain is given in Figures S3–S6 and Table S1. (*) denotes nodes with bootstrap values higher than 70%.

cific polymorphism within *E. huxleyi* (pi = 10.51 $\times$ 10^{-3}, Table 1). *Cox1* (short and long) exhibited the highest intraspecific polymorphism within *G. oceanica* (pi = 10.33 $\times$ 10^{-3} and 8.77 $\times$ 10^{-3}, respectively; Table 1) with a lower level of polymorphism in *E. huxleyi* (pi = 5.15 $\times$ 10^{-3} and 4.90 $\times$ 10^{-3}, respectively; Table 1). *Cox3*, *rpl16* and *dam* all exhibited 0.8%–0.9% intraspecific variability within *E. huxleyi*, but the largest intraspecific divergences for this morpho-species were exhibited by the plastidial *tuf*A (long) and *pet*A markers (1.2% and 1.1% respectively; Table 1).

Phylogenetic patterns. With their lack or relatively low rate of nucleotide substitution, the *18S*, *28S* (nuclear), and *16S* (plastidial) rDNA and the *rbcL* genes were not suitable for constructing phylogenies. Other markers exhibited a phylogenetic signal, in some cases by exclusively selecting parsimonious informative sites. Overall, plastidial and mitochondrial markers generated partially con-

gruent phylogenetic scenarios, with full monophyletic delineation of morpho-species only achieved with the mitochondrial markers (Fig. 1 and Figs. S3–S6 in the Supporting Information). For the plastidial markers, four statistically supported clades were defined the *tuf*A topology, similar to the clades inferred in Cook et al. (2011), while three clades were formed in the *pet*A topology, but in both cases with a clear paraphyletic pattern, with *G. oceanica* strains partly distributed within *E. huxleyi*-dominated clusters (Fig. S3). In detail, the *tuf*A GO clade (Fig. 1) is composed exclusively of *G. oceanica* strains, *tuf*A I contains strains of *E. huxleyi* and *G. oceanica* corresponding to groups 3 and 5 defined by Cook et al. (2011), while *tuf*A II and *tuf*A III contain exclusively *E. huxleyi* and correspond, respectively, to group 1 and groups 2 and 4 of Cook et al. (2011). For both *pet*A and *tuf*A, the phylogenies did not correspond to geographical origin of strains or morpho-species delineation. By contrast, the five mitochondrial markers tested herein displayed consistent phylogenetic patterns with three statistically supported clades and clear morpho-species delineation. Clade γ (Fig. 1) exclusively contains *G. oceanica* strains and is highly diverse in *cox1*. Clades α and β contain the 84 *E. huxleyi* strains analysed, and correspond to the clades described previously and displaying different temperature preferences (α being a warm-water group occurring in the subtropical Atlantic and Pacific and in the Mediterranean Sea and β being a cool-water group occurring in subarctic North Atlantic and North Pacific and in the South Pacific (Beaufort et al. 2011; respectively, clades I and II in Hagino et al. 2011). The diversity within each of these clades differed according to the marker: for example clade β was not well-defined in the *rpl16* phylogeny, while *cox3* showed the highest inter- and intra-clade diversity.

G. oceanica and *E. huxleyi* strains were separated and mitochondrial clades α and β retrieved in the 26 strain tree (Fig. 2) inferred from concatenated sequences of three genes representative of each

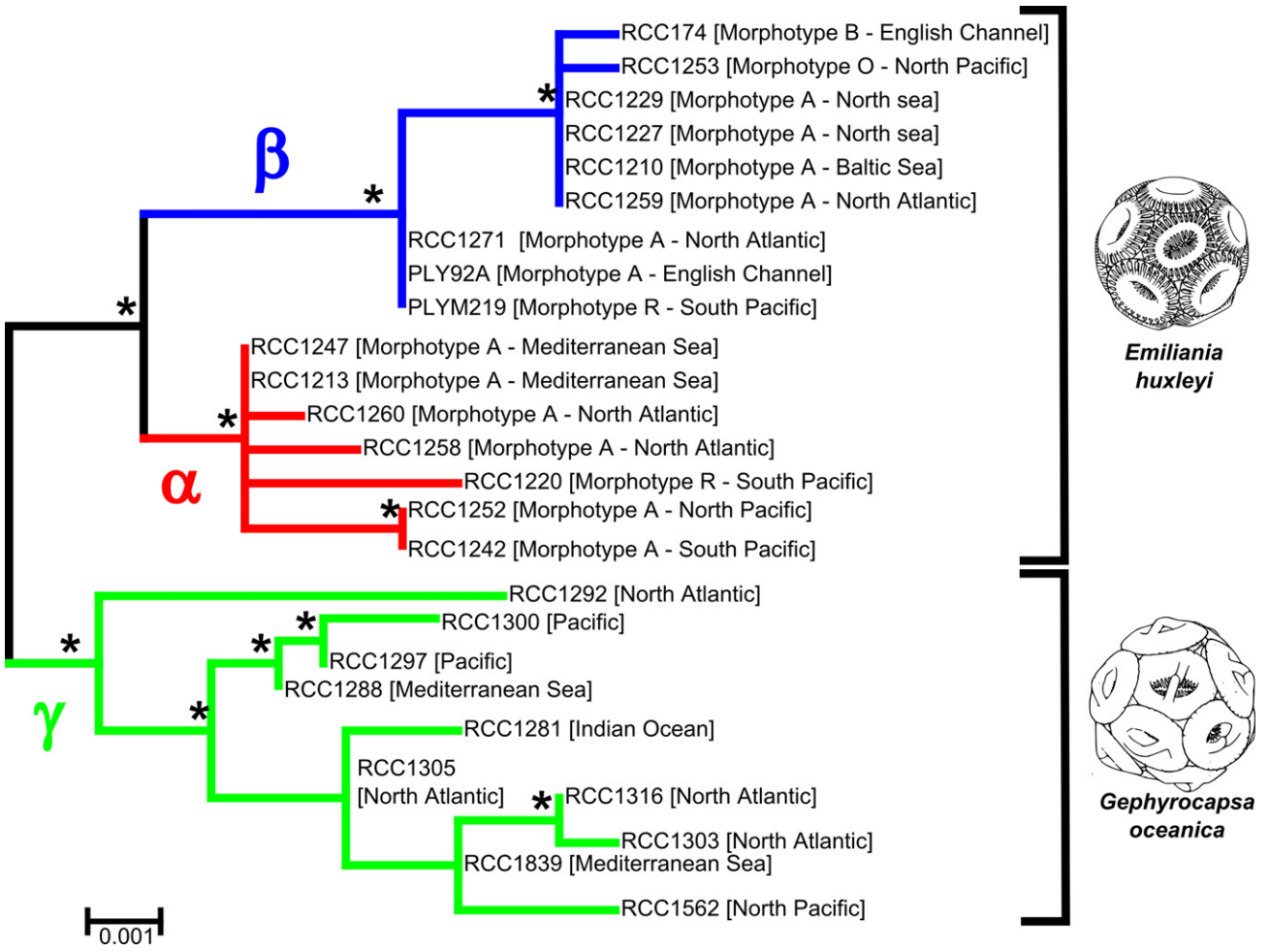

FIG. 2. Unrooted phylogenetic trees inferred from the concatenation of 28S rDNA, *cox1* and *tufA* gene sequences. The pattern of morpho-species delineation is given for the tree according to our SEM observations. (*) denotes nodes with bootstrap values higher than 70%.

genomic compartment (*28S* rDNA, *tufA* and *cox1*). Despite the fact that the two morpho-species were genetically delineated in this analysis, no relationship was found between the genetic grouping and morphotypes within *E. huxleyi*.

DISCUSSION

Gene marker diversity. The comparison of multiple genes in the search for genetic barcodes for accurate species delineation is relatively common for multicellular eukaryotes (plants, animals, and fungi), but has rarely been undertaken for the older and highly diverse protistan lineages (Pawlowski et al. 1997), where nuclear ribosomal DNA markers are still by far the most commonly used barcodes. However, ribosomal genes, occurring in numerous copies in the nuclear genome and interacting with numerous partners during protein synthesis, are under strong purifying selection pressure and are best suited to resolve high-rank relationships due to their slow evolutionary rate and very high level of conservation (Sogin et al. 1986). For marine protists, a particularly high level of conservation of rDNA genes is theoretically expected due to their potentially very high effective population size (Piganeau et al. 2011). Our multigene analysis confirms that rDNAs evolve too slowly to discriminate morpho-species within the *Emiliania/Gephyrocapsa* species complex, which diversified relatively recently during the Quaternary. Likewise, the *16S* rDNA from the plastid genome, also involved in protein synthesis, is highly conserved, as is the *rbcL* gene that codes for the large subunit of RuBisCO and thus plays a central role in carbon fixation by photosynthesis. Neither of these conserved plastid markers are suited for either identification or evolutionary studies of *E. huxleyi/G. oceanica*. However, all other gene markers tested in this study exhibited higher nucleotide substitution rates, with the partial sequences of plastidial *tuf*A (long) and mitochondrial *dam* displaying the highest degrees of variability for the relatively large set of strains analysed, with mean overall substitution rates of, respectively, 6.4% and 6.0% (Table 1).

The general pattern that emerges from our data set is that the plastidial markers do not produce consistent groupings both between and within morpho-species, while the mitochondrial markers delineate a coherent set of genetic clades at both inter- and intra-morpho-species levels. Why such a difference between organelles? Given the fact that the split between *G. oceanica* and *E. huxleyi* occurred only ~291 Kya, the lack of morpho-species segregation by a genetic marker may result from incomplete and differential lineage sorting (i.e., the coalescence point of the given gene predates the speciation event; Maddison and Knowles 2006). However, substitution rates were broadly equivalent between plastidial and mitochondrial gene markers in our data set (Table 1), and thus lineage sorting cannot by itself explain why different organelles present different patterns. Introgression of plastidial genes may be a better explanation. Coccolithophores have a haplo-diplontic sexual life cycle (Billard and Inouye 2004) and the pattern recorded for plastidial markers could reflect past, or even potentially ongoing, hybridization of closely related sublineages of these morpho-species. Introgression of plastid genes is well-documented in plants (e.g. Tsitrone et al. 2003). In many unicellular algae, the plastids from both gametes are present in the newly formed zygote, but the plastid from one mating type typically quickly degenerates (Miyamura 2010). Even in the chlorophyte *Chlamydomonas,* where the plastids from the two gametes fuse, an unknown mechanism leads to uniparental inheritance of plastid DNA (Birky 2008). Although the mode of plastid transmission in the sexual cycle of haptophytes is not known, introgression of plastid genes between recently diverged species remains a possibility.

On the other hand, the reciprocal monophyly between *G. oceanica* and *E. huxleyi* lineages observed in all mitochondrial gene-based phylogenies suggests a mono-parental and uni-directional transmission of this organelle in haptophytes. Transmission of mitochondria in multicellular eukaryotes is typically mono-parental implying that the genealogical history of mitochondrial DNA can be appropriately represented by a unique tree (Avise 2000). Mono-parental mitochondrial transmission has been demonstrated in the green microalga *Chlamydomonas* (Aoyama et al. 2006) and in the brown macroalgal stramenopile *Scytosiphon lomentaria* (Kato et al. 2006), but no experimental data exists for coccolithophores or other haptophytes.

Taxonomic considerations. Overall, the exploration of nuclear, chloroplastic, and mitochondrial markers presented here highlights the extreme relatedness between *G. oceanica* and *E. huxleyi*, that can only be clearly separated using mitochondrial barcodes. This confirms the paleontological data that indicate a relatively recent divergence between these taxa. In addition, *Gephyrocapsa* and *Emiliania* have a strikingly similar life cycle, consisting of a nonmotile placolith-bearing phase ("C-cells"), a motile phase that bears nonmineralized organic scales ("S-cells"), and noncalcified coccoid or amoeboid cells ("N-cells"). The only morphological character that reliably separates the two genera is the loss of calcareous bridge formation in *Emiliania* coccoliths. Note that even if the palaeontological evidence suggests that the *Gephyrocapsa* bridge structure evolved only once, multiple events of bridge gain in pre-*Gephyrocapsa* lineages or of bridge loss in distinct *Gephyrocapsa* lineages cannot be excluded, meaning that reliance on this character for taxonomy at the generic level may well lead to polyphyly. Clearly, these multiple lines of evidence call into question

the validity of the generic level taxonomic differentiation of these taxa.

First described by Lohmann (1902) as *Pontosphaera huxleyi*, *E. huxleyi* has undergone several taxonomic changes through the 20th century (Table S4 in the Supporting Information). The two most recent changes (*Coccolithus* to *Emiliania*, *Emiliania* to *Gephyrocapsa*) represent the crux of the taxonomic question highlighted by the comparative data presented here. Hay and Mohler (Hay et al. 1967) integrated *Coccolithus huxleyi* into a newly erected genus *Emiliania*, even though Kamptner (1956) had noted the high degree of homology of the structure of coccolith elements between *E. huxleyi* and *G. oceanica*. The similarity in coccolith structure of the two species led Reinhardt (1972) to formally propose the transfer of *E. huxleyi* into the genus *Gephyrocapsa*. This proposition has not been widely followed, mainly because, in practice, discrimination of bridge-forming Noëlaerhabdaceae as *Gephyrocapsa* has proven useful, notably for palaeontologists. It can be argued that taxonomic choices should not be dictated by considerations of practical convenience, and the majority of genetic and cytological data supports the transfer of *Emiliania* into the taxonomically older genus *Gephyrocapsa*. Since the combinations *E. huxleyi* and *Gephyrocapsa huxleyi* have both been validly proposed, we conclude that the choice of which name to use is subject to the opinion of individual scientists on this matter, hopefully informed by the data presented here.

Concluding remarks. Our comparative screening of 13 genes from different genomic compartments in 143 coccolithophore strains demonstrated differences in evolutionary modes and rates between the three organellar genomes. Mitochondrial genes combined the best amplification success, sequence quality, and discriminatory power to work within the *Gephyrocapsa/Emiliania* species complex. All mitochondrial markers tested in this study fully distinguished the two morpho-species and provided resolution of microdiversity within the morpho-species. In terms of sequence diversity and phylogenetic signal, *Cox3* appears to be the most promising of these mitochondrial markers for environmental monitoring of these taxa, as already shown in a previous study (Beaufort et al. 2011). The *cox1* gene, by far the most widely used barcode in Metazoa, has slightly lower resolution than *cox3* and has the disadvantage of being separated into two fragments in the mitochondrial genome of *Emiliania* and *Gephyrocapsa* with an intron sometimes present in the larger fragment. Nevertheless, the high level of polymorphism detected in *cox1* sequences of *G. oceanica* could be useful for further studies on the microdiversity within this species.

Our data confirm previous analyses showing that mitochondrial genomes evolve faster than chloroplast genomes in red algal lineages (Smith et al. 2012) and photosynthetic protists with chloroplasts of secondary endosymbiotic origin (Smith and Keeling 2012), in contrast with terrestrial plants and Chlorophyta that exhibit lower substitution rates in mitochondrial compared to chloroplastic DNA. If this holds true for the whole haptophyte lineage and across the SAR super-group (Burki et al. 2007), the conceptual and methodological framework based on mitochondrial markers developed for phylogeographic and barcoding analyses in Metazoa could be applied to assess species diversity and ecology in the largest fraction of protistan biodiversity.

We thank Dr. Antonio Pagarete for providing the *E. huxleyi tuf*A primer sequences. We thank Morgan Perennou and Gwen Tanguy from the GENOMER platform at the Station Biologique de Roscoff for technical assistance with sequencing. We are also grateful to Jeremy Young for helpful discussions and the two anonymous reviewers for their constructive comments. This work was supported by the European Research Council under the European Community's Seventh Framework Programme (EC-FP7) through the European Project on Ocean Acidification (EPOCA, grant agreement 211384; EMB), a Marie Curie Intra-European Fellowship (grant FP7-PEOPLE-2012-IEF; EMB), ASSEMBLE (grant 227 799; IP), the Interreg IV program MARINEXUS the EU EraNet BiodivERsA program "Biodiversity of Marine euKaryotes (BioMarKs; SR), and by the "Investissements d'Avenir" project w*O*rld o*CEAN* bi*O*ressources, biotechnologies, and Earth-syste*M* serv*ICeS* (OCEANOMICS; CdV).

Aoyama, H., Hagiwara, Y., Misumi, O., Kuroiwa, T. & Nakamura, S. 2006. Complete elimination of maternal mitochondrial DNA during meiosis resulting in the paternal inheritance of the mitochondrial genome in *Chlamydomonas* species. *Protoplasma* 228:231–42.

Avise, J. C. 2000. *Phylogeography: The History and Formation of Species*. Harvard University Press, Cambridge, 447 pp.

Beaufort, L., Probert, I., de Garidel-Thoron, T., Bendif, E.M., Ruiz-Pino, D., Metzl, N., Goyet, C., et al. 2011. Sensitivity of coccolithophores to carbonate chemistry and ocean acidification. *Nature* 476:80–3.

Billard, C. & Inouye, I. 2004. What's new in coccolithophore biology? *In* Thierstein, H. R. & Young, J. R. [Eds.] *Coccolithophores – From Molecular Processes to Global Impact*. Springer, Berlin, pp. 1–30.

Birky, C. W. 2008. Uniparental inheritance of organelle genes. *Curr. Biol.* 18:692–5.

Blackburn, S. I. & Cresswell, G. 1993. A coccolithophorid bloom in Jervis Bay, Australia. *Aust. J. Mar. Freshwater Res.* 44:253–60.

Bown, P. R. 2005. Calcareous nannoplankton evolution: a tale of two oceans. *Micropaleontology* 51:299–308.

Burki, F., Shalchian-Tabrizi, K., Minge, M. A., Skjaeveland, A., Nikolaev, S. I., Jakobsen, K. S. & Pawlowski, J. 2007. Phylogenomics reshuffles the eukaryotic supergroups. *PLoS ONE* 2: e790.

Candelier, Y., Minoletti, F., Probert, I. & Hermoso, M. 2013. Temperature dependence of oxygen isotope fractionation in coccolith calcite: a culture and core top calibration of the genus *Calcidiscus*. *Geo. Cosmo. Acta* 100:264–81.

Cook, S. S., Whittock, L., Wright, S. W. & Hallegraeff, G. M. 2011. Photosynthetic pigment and genetic differences between two Southern Ocean morphotypes of *Emiliania huxleyi* (Haptophyta). *J. Phycol.* 47:615–26.

Edvardsen, B., Eikrem, W., Green, J. C., Andersen, R. A., Moon-van der Staay, S. Y. & Medlin, L. K. 2000. Phylogenetic reconstructions of the Haptophyta inferred from 18S ribosomal DNA sequences and available morphological data. *Phycologia* 39:19–35.

Fujiwara, S., Tsuzuki, M., Kawachi, M., Minaka, N. & Inouye, I. 2001. Molecular phylogeny of the Haptophyta based on the

rbcL gene and sequence variation in the spacer region of the RUBISCO operon. *Phycologia* 37:121–9.

Hagino, K., Bendif, E. M., Young, J., Kogame, K., Takano, Y., Probert, I., Horiguchi, T., de Vargas, C. & Okada, H. 2011. New evidence for morphological and genetic variation in the cosmopolitan coccolithophore Emiliana huxleyi (Prymnesiophyceae) from the cox1b-ATP4 genes. *J. Phycol.* 47: 1164–76.

Hall, T. A. 1999. BioEdit: a user-friendly biological sequence alignment editor and analysis program for Windows 95/98/NT. *Nucl. Acids Symp. Ser.* 4:95–8.

Hasegawa, M., Kishino, H. & Yano, T. 1985. Dating the human-ape splitting by a molecular clock of mitochondrial DNA. *J. Mol. Evol.* 22:160–174.

Hay, W. W., Mohler, H. P., Roth, P. H., Schmidt, R. R. & Boudreaux, J. E. 1967. Calcareous nannoplankton zonation of the Cenozoic of the Gulf Coast and Caribbean-Antillean area, and transoceanic correlation. *Trans. Gulf. Coast. Asso. Geol. Soc.* 17:428–80.

Iglesias-Rodriguez, M. D., Halloran, P. R., Rickaby, R. E. M., Hall, I. R., Colmenero-Hidalgo, E., Gittins, J. R., Green, D. R. H. et al. 2008. Phytoplankton calcification in a high-CO_2 world. *Science* 320:336–40.

Kai, M., Hara, T., Aoyama, H. & Kuroda, N. 1999. A massive coccolithophorid bloom observed in Mikawa Bay, Japan. *J. Ocean.* 55:395–406.

Kamptner, E. 1943. Zur Revision der Coccolithineen-Spezies *Pontosphaera huxleyi* Lohmann. *Anz. Akad. Wiss. Wien. Math. –Naturw. K.* 80:43–9.

Kamptner, E. 1956. Das Kalkskelett von *Coccolithus huxleyi* (Lohmann) Kamptner und *Gephyrocapsa oceanica* Kamptner (Coccolithineae). *Arch. Protistenkd.* 101:99–202.

Kato, Y., Kogame, K., Nagasato, C. & Motomura, T. 2006. Inheritance of mitochondrial and chloroplast genomes in the isogamous brown alga *Scytosiphon lomentaria* (Phaeophyceae). *Phycol. Res.* 54:65–71.

Katoh, K., Kuma, K., Toh, H. & Miyata, T. 2007. MAFFT version 5: improvement in accuracy of multiple sequence alignment. *Nucleic Acids Res.* 33:511–8.

Keller, M. D., Selvin, R. C., Claus, W. & Guillard, R. R. L. 1987. Media for the culture of oceanic ultraphytoplankton. *J. Phycol.* 23:633–8.

Kimura, M. 1980. A simple method for estimating evolutionary rates of base substitutions through comparative studies of nucleotide sequences. *J. Mol. Evol.* 16:111–20.

Langer, G., Nehrke, G., Probert, I., Ly, J. & Ziveri, P. 2009. Strain-specific responses of *Emiliania huxleyi* to changing seawater carbonate chemistry. *Biogeosciences* 6:2637–46.

Librado, P. & Rozas, J. 2009. DnaSP v5: a software for comprehensive analysis of DNA polymorphism data. *Bioinformatics* 25:1451–2.

Liu, H., Aris-Brosou, S., Probert, I. & de Vargas, C. 2010. A timeline of the environmental genetics of the haptophytes. *Mol. Biol. Evol.* 27:171–6.

Lohmann, H. 1902. Die Coccolithophoridae, eine monographie der Coccolithen bildenden flagellaten, zugleich ein Beitag zur Kenntnis des Mittelmeerauftriebs. *Arch. Protistenkde.* 1: 89–165.

Maddison, W. P. & Knowles, L. L. 2006. Inferring phylogeny despite incomplete lineage sorting. *Syst. Biol.* 55:21–30.

Medlin, L. K., Sàez, A. G. & Young, J. R. 2008. A molecular clock for coccolithophores and implications for selectivity of phytoplankton extinctions across the K/T boundary. *Mar. Micropal.* 67:69–86.

Miyamura, S. 2010. Cytoplasmic inheritance in green algae: patterns, mechanisms and relation to sex type. *J. Plant. Res.* 123:171–84.

Müller, P. J., Kirst, G., Ruhland, G., von Storch, I. & Rosell-Mele, A. 1998. Calibration of the alkenone paleotemperature index UK'37 based on core-tops from the eastern South Atlantic and the global ocean (60°N–60°S). *Geochim. Cosmochim. Acta* 62:1757–72.

Nei, M. 1987. *Molecular Evolutionary Genetics.* Columbia University Press, New York.

Pawlowski, J., Bolivar, I., Fahrni, J. F., de Vargas, C., Gouy, M. & Zaninetti, L. 1997. Extreme differences in rates of molecular evolution of foraminifera revealed by comparison of ribosomal DNA sequences and the fossil record. *Mol. Biol. Evol.* 14:498–505.

Piganeau, G., Eyre-Walker, A., Grimsley, N. & Moreau, H. 2011. How and why DNA barcodes underestimate the diversity of microbial eukaryotes. *PLoS ONE* 6:e16342.

Raffi, I., Backman, J., Fornaciari, E., Pälike, H., Domenico, R. H., Lourens, L. & Hilgen, F. 2006. A review of calcareous nannofossil astrobiochronology encompassing the past 25 million years. *Quat. Sci. Rev.* 25:3113–3137.

Reinhardt, P. 1972. Coccolithen. Kalkiges Plankton seit Jahrmillionen. *Die neue Brehm. Bücheri.* 453:1–99.

Riebesell, U., Zondervan, I., Rost, B., Tortell, P. D., Zeebe, R. E. & Morel, F. M. M. 2000. Reduced calcification of marine plankton in response to increased atmospheric CO_2. *Nature* 407:364–7.

Rost, B. & Riebesell, U. 2004. Coccolithophores and the biological pump responses to environmental changes. *In* Thierstein, H. R. & Young, J. R. [Eds.] *Coccolithophores – From Molecular Processes to Global Impact.* Springer, Berlin, pp. 99–125.

Samtleben, C. 1980. Die evolution der coccolithophoriden-Gattung *Gephyrocapsa* nach Befunden im Atlantik. *Pal. Zeit.* 54:91–127.

Sánchez Puerta, V., Bachvaroff, T. R. & Delwiche, C. F. 2004. The complete Mitochondrial genome sequence of the Haptophyte *Emiliania huxleyi* and its Relation to Heterokonts. *DNA Res.* 11:1–10.

Sanchez-Puerta, M. V., Bachvaroff, T. R. & Delwiche, C. F. 2005. The complete plastid genome sequence of the haptophyte *Emiliania huxleyi*: a comparison to other plastid genomes. *DNA Res.* 12:151–6.

Schroeder, D. C., Biggi, G. F., Hall, M., Davy, J., Martínez, J. M., Richardson, A. J., Malin, G. & Wilson, W. H. 2005. A genetic marker to separate *Emiliania huxleyi* (Prymnesiophyceae) morphotypes. *J. Phycol.* 41:874–9.

Smith, D. R., Hua, J., Lee, R. W. & Keeling, P. J. 2012. Relative rates of evolution among the three genetic compartments of the red alga Porphyra differ from those of green plants and do not correlate with genome architecture. *Mol. Phylogenet. Evol.* 65:339–4.

Smith, D. R. & Keeling, P. J. 2012. Twenty-fold difference in evolutionary rates between the mitochondrial and plastid genomes of species with secondary red plastids. *J. Eukaryot. Microbiol.* 59:181–4.

Sogin, M. L., Elwood, H. J. & Gunderson, J. H. 1986. Evolutionary diversity of eukaryotic small-subunit rRNA genes. *Proc. Natl. Acad. Sci. USA* 83:1383–7.

Tamura, K. & Nei, M. 1993. Estimation of the number of nucleotide substitutions in the control region of mitochondrial DNA in humans and chimpanzees. *Mol. Biol. Evol.* 10:512–26.

Tamura, K., Peterson, D., Peterson, N., Stecher, G., Nei, M. & Kumar, S. 2011. MEGA5: molecular evolutionary genetics analysis using maximum likelihood, evolutionary distance, and maximum parsimony methods. *Mol. Biol. Evol.* 28: 2731–9.

Tsitrone, A., Kirkpatrick, M., Levin, D. A. & Morgan, M. 2003. A model for chloroplast capture. *Evolution* 57:1776–82.

Winter, A., Jordan, R. & Roth, P. 1994. Biogeography of living coccolithophores in ocean waters. *In* Winter, A. & Siesser, W. G. [Eds.] *Coccolithophores.* Cambridge University Press, Cambridge, pp. 161–77.

Supporting Information

Additional Supporting Information may be found in the online version of this article at the publisher's web site:

Figure S1. SEM images of *Gephyrocapsa oceanica* (left) and *Emiliania huxleyi* (right).

Figure S2. Primer mapping for each of the markers used in this study.

Figure S3. Phylogenetic trees inferred from plastid genes *tuf*A and *pet*A. In the *tuf*A (short) tree, orange corresponds to a clade with strains from clade *tuf*A I and clade *tuf*A II. Green dots correspond to *Gephyrocapsa oceanica*.

Figure S4. Phylogenetic trees inferred from mitochondrial gene *cox1* (long and short fragments). In the *cox1* (short) tree, green dots correspond to *Gephyrocapsa oceanica*.

Figure S5. Phylogenetic trees inferred from mitochondrial genes *cox2* and *cox3*.

Figure S6. Phylogenetic trees inferred from mitochondrial genes *rpl16* and *dam*.

Table S1. List of strains used in this study with their designations and genetic characterization. (EH and GO: respectively, 28S ribotype *Emiliania huxleyi* and *Gephyrocapsa oceanica*, N: Noelaerhabdaceae; Identical sequences).

Table S2. Details of genetic markers and primers used in this study.

Table S3. Genbank accession numbers.

Table S4. Genus level taxonomic changes in the morpho-species *Emiliania huxleyi*.